

A new basis for filament simulation in three dimensions

Benjamin J. Walker,^{1,*} Kenta Ishimoto,^{2,†} and Eamonn A. Gaffney^{1,‡}

¹*Wolfson Centre for Mathematical Biology, Mathematical Institute, University of Oxford, Oxford, OX2 6GG, UK*

²*Graduate School of Mathematical Sciences, The University of Tokyo, Tokyo, 153-8914, Japan*

(Dated: July 5, 2019)

Simulations of slender inextensible filaments in a viscous fluid are often plagued by numerical stiffness. Recent coarse-graining studies have reduced the computational requirements of such systems, though have thus far been limited to the motion of planar filaments. In this work we extend such frameworks to filament motion in three dimensions, identifying and circumventing artificial singularities introduced by filament parameterisation via repeated changes of basis. The resulting methodology enables efficient and rapid study of the motion of flexible filaments in three dimensions, and is readily extensible to a wide range of problems, including filament motion in confined geometries, large-scale active matter simulations, and the motility of mammalian spermatozoa.

PACS numbers: 47.15.G-, 47.63.Gd, 87.15.La

INTRODUCTION

The coupled elastohydrodynamics of flexible filaments on the microscale are of significance to much of biology [1–3], in addition to being of pertinence to the development of microdevices and interaction of flows near surfaces [4, 5]. The complex mechanics of fluid-structure interaction has been well studied, as illustrated by the slender body theory of Tornberg and Shelley [6] and Liu *et al.* [7] and the boundary element computations of Pozrikidis [8]. Necessary to the numerical study of filament mechanics is an appropriate framework, capable of realising efficient simulation of coupled filament elastohydrodynamics, as noted in the recent extensive review of du Roure *et al.* [9]. To this end, in this work we develop and implement a framework for the solution of the elastohydrodynamics of an inextensible, unshearable filament in three spatial dimensions, attempting to circumvent the extreme numerical stiffness typically associated with the mechanics of filaments in a viscous fluid. Recent developments in this field include the work of Schoeller *et al.* [10], which utilises a quaternion representation of filament orientation to parameterise the three dimensional shape of the slender body, additionally making use of the force coupling method [11]. In the framework of Schoeller *et al.* [10] significant numerical care is required to satisfy the condition of filament inextensibility, thus there is scope for the development of an accurate modelling framework that circumvents the computational work typically needed to satisfy this constraint.

A core motivation for developing this framework is the mechanics of filaments used to drive cellular swimming, in particular the sperm flagellum. This readily exhibits three dimensional motions and despite difficulties in experimentally observing the flagellum at the resolution necessary to draw conclusions about its internal mechanics, the evidence is that the mammalian flagellum does not twist during non-planar motions

[12]. This is also further supported by studies of sea urchin, the ‘E. Coli’ for flagellum studies, where rotations of the flagellar beat plane induced experimentally are not accompanied by flagellar twist [13]. Furthermore, previous studies of the fluid-structure coupling between sperm-flagella and the surrounding fluid have been plagued by extreme numerical stiffness, to the extent that practical simulation studies have been limited and parameter space studies are all but prohibitive [14, 15]. Hence, our fundamental objective is to develop a simulation framework for studying the mechanics of a general twistable rod that can bend in any direction, and showcase its flexibility by considering the special case of an untwistable filament. Further, we aim to present such a framework that also circumvents the extreme numerical stiffness of earlier developments to enable the study of large parameter spaces and collective behaviour in the physics of swimming cells, and in turn cellular active matter.

In this study we will seek to extend the recent work of Moreau *et al.* [16], Walker *et al.* [17], Hall-McNair *et al.* [18] to three dimensions, attempting to retain the reduction in numerical stiffness offered by their methodologies. Further to considering motion in three dimensions, we will also aim to include a model of non-local hydrodynamics as in Ishimoto and Gaffney [15] and Olson *et al.* [14], utilising the method of regularised Stokeslet segments as introduced by Cortez [19] to obtain high-accuracy solutions of the coupled elastohydrodynamics. We aim to cast the elastohydrodynamical problem in such a way as to be readily solvable by existing numerical methods, and further such that it is extensible to a variety of modelling problems, from clamped filaments in flow as studied by Pozrikidis [8], Walker *et al.* [17] to the collective motion of active filaments.

METHODS

Equations of elasticity

We consider a slender inextensible unshearable filament in a viscous Newtonian fluid with centreline described by $\mathbf{x}(s)$, parameterised by arclength $s \in [0, L]$ for filament length L . Here and throughout, the Reynolds number will be taken to be identically zero. Along the filament we have the pointwise conditions of force and moment balance, given explicitly by

$$\mathbf{n}_s - \mathbf{f} = \mathbf{0}, \quad (1)$$

$$\mathbf{m}_s + \mathbf{x}_s \times \mathbf{n} - \boldsymbol{\tau} = \mathbf{0}, \quad (2)$$

for contact force and couple denoted \mathbf{n}, \mathbf{m} respectively and where a subscript of s denotes differentiation with respect to arclength. The quantity \mathbf{f} is the force per unit length applied on the fluid medium by the filament, which we will later express in terms of the filament velocity $\dot{\mathbf{x}}$, where here dot denotes a time derivative. Similarly, $\boldsymbol{\tau}$ is the torque per unit length applied on the fluid medium by the rotation of the filament. Following the approach of Moreau *et al.* [16], integrating these pointwise balance equations under the assumptions of zero contact force and couple at the tip of the filament yields the integrated balance equations

$$-\int_s^L \mathbf{f}(s) ds = \mathbf{n}(0), \quad (3)$$

$$-\int_s^L [(\mathbf{x}(\tilde{s}) - \mathbf{x}(s)) \times \mathbf{f}(\tilde{s}) + \boldsymbol{\tau}(\tilde{s})] d\tilde{s} = \mathbf{m}(s). \quad (4)$$

Given a right-handed orthonormal basis $\{\mathbf{d}_1(s), \mathbf{d}_2(s), \mathbf{d}_3(s)\}$ such that \mathbf{d}_3 corresponds to the local filament tangent, following the approach of Nizette and Goriely [20] for $\alpha = 1, 2, 3$ we define the twist vector $\boldsymbol{\kappa}$ by

$$\frac{\partial \mathbf{d}_\alpha}{\partial s} = \boldsymbol{\kappa} \times \mathbf{d}_\alpha. \quad (5)$$

Writing $\boldsymbol{\kappa} = \sum_\alpha \kappa_\alpha \mathbf{d}_\alpha$, for bending stiffness EI we adopt a linear constitutive relation between the torque \mathbf{m} and the twist vector $\boldsymbol{\kappa}$, which

$$\mathbf{m} = EI \left(\kappa_1 \mathbf{d}_1 + \kappa_2 \mathbf{d}_2 + \frac{1}{1 + \sigma} \kappa_3 \mathbf{d}_3 \right), \quad (6)$$

where σ is the Poisson ratio [20]. With this constitutive relation the integrated moment balance equations in the \mathbf{d}_1 and \mathbf{d}_2 directions are simply

$$\begin{aligned} -\mathbf{d}_\alpha(s) \cdot \int_s^L [(\mathbf{x}(\tilde{s}) - \mathbf{x}(s)) \times \mathbf{f}(\tilde{s}) + \boldsymbol{\tau}(\tilde{s})] d\tilde{s} \\ = \frac{EI}{1 + \delta_{\alpha,3}\sigma} \kappa_\alpha(s), \end{aligned} \quad (7)$$

for $\alpha = 1, 2, 3$ and $\delta_{\alpha,b}$ denotes the Kronecker delta.

Filament discretisation

In discretising the filament we follow the approach of Walker *et al.* [17], as previously applied to planar filaments and itself building upon the earlier work of Moreau *et al.* [16]. We approximate the filament with N piecewise-linear segments, each of constant length Δs , with segment endpoints having positions denoted by $\mathbf{x}_1, \dots, \mathbf{x}_{N+1}$ and the inextensibility constraint satisfied inherently. The endpoints of the i^{th} segment correspond to \mathbf{x}_i and \mathbf{x}_{i+1} for $i = 1, \dots, N$, with the local tangent \mathbf{d}_3 being constant on each segment and denoted \mathbf{d}_3^i . In what follows we will consider a choice of $\mathbf{d}_1, \mathbf{d}_2$ such that they are also constant on each segment, without loss of generality, and we denote these constants similarly as $\mathbf{d}_1^i, \mathbf{d}_2^i$. Writing s_i for the constant arclength associated with each material point \mathbf{x}_i , we apply Eq. (7) at each of the s_i for $i = 1, \dots, N$, splitting the integral at the segment endpoints to give

$$\begin{aligned} -\mathbf{d}_\alpha^i \cdot \sum_{j=i}^N \int_{s_j}^{s_{j+1}} [(\mathbf{x}(\tilde{s}) - \mathbf{x}_i) \times \mathbf{f}(\tilde{s}) + \boldsymbol{\tau}(\tilde{s})] d\tilde{s} \\ = \frac{EI}{1 + \delta_{\alpha,3}\sigma} \kappa_\alpha(s_i), \end{aligned} \quad (8)$$

for $\alpha = 1, 2$. On the j^{th} segment, \mathbf{x} may be written as $\mathbf{x}(s) = \mathbf{x}_j + \eta(\mathbf{x}_{j+1} - \mathbf{x}_j)$, where $\eta \in [0, 1]$ is given by $\eta = (s - s_j)/\Delta s$. Additionally, discretising the force per unit length as a continuous piecewise-linear function, with η as above we have $\mathbf{f}(s) = \mathbf{f}_j + \eta(\mathbf{f}_{j+1} - \mathbf{f}_j)$ on the segment, where we write $\mathbf{f}_j = \mathbf{f}(s_j)$. Substitution of these parameterisations into Eq. (8) and subsequent integration yields, after simplification,

$$-\mathbf{d}_\alpha^i \cdot \left(\mathbf{I}_i^f + \mathbf{I}_i^\tau \right) \Delta s = \frac{EI}{1 + \delta_{\alpha,3}\sigma} \kappa_\alpha(s_i), \quad (9)$$

where the integral contribution of the force and torque densities are denoted \mathbf{I}_i^f and \mathbf{I}_i^τ respectively. With this discretisation \mathbf{I}_i^f has reduced to

$$\begin{aligned} \left[\frac{1}{2}(\mathbf{x}_N - \mathbf{x}_i) + \frac{\Delta s}{3} \mathbf{d}_3^i \right] \times \mathbf{f}_{N+1} \\ + \sum_{j=i+1}^N \left[(\mathbf{x}_j - \mathbf{x}_i) + \frac{\Delta s}{2} \mathbf{d}_3^j \right] \times \mathbf{f}_j \\ + \frac{\Delta s}{6} \mathbf{d}_3^i \times \mathbf{f}_i. \end{aligned} \quad (10)$$

For \mathbf{I}_i^τ we consider a piecewise constant discretisation of the torque per unit length, taking $\boldsymbol{\tau} = \boldsymbol{\tau}_j$ on the j^{th}

segment. This yields the simple expression

$$\mathbf{I}_i^\tau = \sum_{j=i}^N \boldsymbol{\tau}_j, \quad (11)$$

where we note that the Δs term expected from the integral has been factored out in Eq. (9).

From the above we see explicitly that the integral component of each moment balance equation may be written as a linear operator on the \mathbf{f}_j and the $\boldsymbol{\tau}_j$, noting that the cyclic property of the scalar triple product further simplifies the vector products in the above representation.

Similarly, with this piecewise-linear discretisation the integrated force balance of Eq. (3) simply reads

$$-\frac{\Delta s}{2} \sum_{j=1}^N (\mathbf{f}_j + \mathbf{f}_{j+1}) = \mathbf{n}(0). \quad (12)$$

We write $\mathbf{F} = [f_{1,x}, f_{1,y}, f_{1,z}, \dots, f_{N+1,x}, f_{N+1,y}, f_{N+1,z}]^\top$ for components $f_{j,x}, f_{j,y}, f_{j,z}$ of \mathbf{f}_j with respect to some fixed laboratory frame with basis $\{\mathbf{e}_x, \mathbf{e}_y, \mathbf{e}_z\}$, and similarly \mathbf{T} for the vector of components of torque per unit length. With this notation we may write the equations of force and moment balance as

$$-\mathcal{B}\mathbf{F} = \mathbf{R}, \quad (13)$$

where \mathcal{B} is a matrix of dimension $(3N+3) \times (6N+3)$ with rows \mathcal{B}_k . For $k = 1, 2, 3$ these are given by

$$\begin{aligned} \mathcal{B}_1 &= \frac{\Delta s}{2} [1, 0, 0, 2, 0, 0, 2, \dots, 2, 0, 0, 1, 0, 0], \\ \mathcal{B}_2 &= \frac{\Delta s}{2} [0, 1, 0, 0, 2, 0, 0, 2, \dots, 2, 0, 0, 1, 0], \\ \mathcal{B}_3 &= \frac{\Delta s}{2} [0, 0, 1, 0, 0, 2, 0, 0, 2, \dots, 2, 0, 0, 1], \end{aligned} \quad (14)$$

and correspond to the force balance equation Eq. (12). The remaining rows of \mathcal{B} encode the moment balance of Eq. (9), organised in pairs such that $\mathcal{B}_{2(i-1)+3+\alpha}$ corresponds to the α^{th} component of the i^{th} moment balance equation. Accordingly, and under the assumption of a force-free filament base, the $(2N+3)$ -vector \mathbf{R} is given by

$$\mathbf{R} = \frac{EI}{\Delta s} [0, 0, 0, \kappa_1(s_1), \kappa_2(s_1), \kappa_1(s_2), \dots, \kappa_2(s_N)]^\top. \quad (15)$$

We remark that each of the quantities involved in the construction of \mathcal{B} and \mathbf{R} are well-defined for a general filament in three dimensions, subject to a choice of \mathbf{d}_1 and \mathbf{d}_2 and computing the components of the twist vector as $\kappa_1 = \mathbf{d}_3 \cdot \partial_s \mathbf{d}_2$, $\kappa_2 = \mathbf{d}_1 \cdot \partial_s \mathbf{d}_3$, and $\kappa_3 = \mathbf{d}_2 \cdot \partial_s \mathbf{d}_1$. Additionally, we will proceed assuming that the filament is moment-free at the base, which additionally enforces $\kappa_1(0) = \kappa_2(0) = \kappa_3(0) = 0$.

Coupling hydrodynamics

We now relate the force density \mathbf{f} acting on the fluid to the velocity of each segment endpoint, utilising the method of regularised Stokeslet segments as introduced by Cortez [19] and adopted by Walker *et al.* [17] for planar filaments. Here taking regularisation parameter $\epsilon = 10^{-3}L$ to represent the filament radius, as justified by Cortez [19], the method of regularised Stokeslet segments considers a piecewise linear distribution of regularised Stokeslets along straight segments in three dimensions, and hence may be directly applied to our discretised filament. With our notation consistent with that of section 2.2 of Walker *et al.* [17], we direct the reader to this previous work for a full derivation of the non-local coupling between filament velocities and applied force density. We remark that we will consider only free-space hydrodynamics, and in this work do not include a planar boundary, though our presented methodology is readily extensible to such confined geometries. Summarising section 2.2 of Walker *et al.* [17], we may write

$$\dot{\mathbf{X}} = A\mathbf{F}, \quad (16)$$

where A is a square matrix of dimension $3(N+1) \times 3(N+1)$ and is a function only of the segment endpoints \mathbf{x}_i . Of dimension $3(N+1)$, the vector $\dot{\mathbf{X}}$ corresponds to the velocities of the segment endpoints, and is constructed analogously to \mathbf{F} with respect to the laboratory frame. This relation results from the application of the no-slip condition at the segment endpoints, coupling the filament to the surrounding fluid.

In order to relate the rate of rotation of each segment to the viscous torque $\boldsymbol{\tau}_i$ acting on it, we here consider an approximation of the finite segment as an infinite rotating cylinder, associating the torque per unit length on the i^{th} segment with the rotation ω_i about its local tangent \mathbf{d}_3^i via the relation of Chwang and Wu [21]:

$$\boldsymbol{\tau}_i = 4\pi\mu\epsilon^2\omega_i\mathbf{d}_3^i. \quad (17)$$

Here μ is the viscosity of the fluid medium, and we recall that ϵ is the radius of the filament. We may write this relation as a linear operator on $\boldsymbol{\omega} = [\omega_1, \dots, \omega_N]^\top$, written simply as $\mathbf{T} = \tilde{A}\boldsymbol{\omega}$. This crude approximation may readily be substituted for non-local hydrodynamics via the method of regularised Stokeslet segments, which will likely be a topic of future work.

Combining Eqs. (13), (16) and (17) yields the linear system

$$-\mathcal{B} \begin{bmatrix} A^{-1} & 0 \\ 0 & \tilde{A} \end{bmatrix} \begin{bmatrix} \dot{\mathbf{X}} \\ \boldsymbol{\omega} \end{bmatrix} = -\mathcal{B}\mathcal{A} \begin{bmatrix} \dot{\mathbf{X}} \\ \boldsymbol{\omega} \end{bmatrix} = \mathbf{R}, \quad (18)$$

where we are assuming that A is invertible and defining \mathcal{A} to be a block matrix of dimension $(6N+3) \times (4N+3)$ with non-zero blocks A^{-1} and \tilde{A} .

Parameterisation

We may parameterise the tangents \mathbf{d}_3^i on each linear segment by the Euler angles $\theta_i \in [0, \pi]$, $\phi_i \in (-\pi, \pi]$ for $i = 1, \dots, N$ [22]. With this parameterisation we may make a choice of \mathbf{d}_1 and \mathbf{d}_2 , taking here the three orthonormal vectors to be

$$\mathbf{d}_1^i = [-s_\phi c_\psi - c_\theta c_\phi s_\psi, +c_\phi c_\psi - c_\theta s_\phi s_\psi, s_\theta s_\psi]^\top, \quad (19)$$

$$\mathbf{d}_2^i = [+s_\phi s_\psi - c_\theta c_\phi c_\psi, -c_\phi s_\psi - c_\theta s_\phi c_\psi, s_\theta c_\psi]^\top, \quad (20)$$

$$\mathbf{d}_3^i = [s_\theta c_\phi, s_\theta s_\phi, c_\theta]^\top, \quad (21)$$

written with respect to the laboratory frame and where $s_\theta \equiv \sin \theta_i$, $c_\theta \equiv \cos \theta_i$, and analogously for s_ϕ , c_ϕ , s_ψ and c_ψ . From the directors we recover

$$\theta_i = \arccos(\mathbf{d}_3^i \cdot \mathbf{e}_z), \quad (22)$$

$$\phi_i = \arctan\left(\frac{\mathbf{d}_3^i \cdot \mathbf{e}_y}{\mathbf{d}_3^i \cdot \mathbf{e}_x}\right), \quad (23)$$

$$\psi_i = \arctan\left(\frac{\mathbf{d}_1^i \cdot \mathbf{e}_z}{\mathbf{d}_2^i \cdot \mathbf{e}_z}\right). \quad (24)$$

As the discretised filament is piecewise linear, for $j = 1, \dots, N + 1$ we may write

$$\mathbf{x}_j = \mathbf{x}_1 + \Delta s \sum_{i=1}^{j-1} \mathbf{d}_3^i, \quad (25)$$

$$\dot{\mathbf{x}}_j = \dot{\mathbf{x}}_1 + \Delta s \sum_{i=1}^{j-1} \dot{\mathbf{d}}_3^i. \quad (26)$$

With \mathbf{d}_3^i parameterised as above, we can thus express $\dot{\mathbf{x}}_j$ as a linear combination of the derivatives of θ_i , and ϕ_i for $i = 1, \dots, j - 1$, in addition to including the time derivative of the base point \mathbf{x}_1 . Hence we may write

$$\mathcal{Q} \dot{\Theta} = \dot{\mathbf{X}}, \quad (27)$$

$$\Theta = [x_{1,x}, x_{1,y}, x_{1,z}, \theta_1, \dots, \theta_N, \phi_1, \dots, \phi_N]^\top, \quad (28)$$

where \mathcal{Q} is a $3(N+1) \times (2N+3)$ matrix and $x_{j,x}, x_{j,y}, x_{j,z}$ are the components of \mathbf{x}_j in the basis $\{\mathbf{e}_x, \mathbf{e}_y, \mathbf{e}_z\}$. Explicitly, \mathcal{Q} may be constructed as

$$\mathcal{Q} = \left[\begin{array}{c|c|c} Q_{11} & Q_{12} & Q_{13} \\ \hline Q_{21} & Q_{22} & Q_{23} \\ \hline Q_{31} & Q_{32} & Q_{33} \end{array} \right]_P, \quad (29)$$

where the matrices Q_{k1} are of dimension $(N+1) \times 3$, with Q_{k2} and Q_{k3} being of dimension $(N+1) \times N$, for $k = 1, 2, 3$. The subscript P denotes that the i^{th} row of \mathcal{Q} is to be permuted to

$$P(i) = \begin{cases} 3(i-1) + 1, & i = 1, \dots, N+1, \\ 3(i-N-2) + 2, & i = N+2, \dots, 2N+2, \\ 3(i-2N-3) + 3, & i = 2N+3, \dots, 3N+3. \end{cases} \quad (30)$$

This permutation of \mathcal{Q} allows us to define the sub-blocks of \mathcal{Q} simply, given explicitly as

$$\begin{aligned} Q_{k1}^{i,j} &= \begin{cases} 1, & j = k, \\ 0, & \text{otherwise,} \end{cases} \quad k = 1, 2, 3, \\ Q_{12}^{i,j} &= \Delta s \begin{cases} +\cos \theta_j \cos \phi_j, & j < i, \\ 0, & j \geq i, \end{cases} \\ Q_{13}^{i,j} &= \Delta s \begin{cases} -\sin \theta_j \sin \phi_j, & j < i, \\ 0, & j \geq i, \end{cases} \\ Q_{22}^{i,j} &= \Delta s \begin{cases} +\cos \theta_j \sin \phi_j, & j < i, \\ 0, & j \geq i, \end{cases} \\ Q_{23}^{i,j} &= \Delta s \begin{cases} +\sin \theta_j \cos \phi_j, & j < i, \\ 0, & j \geq i, \end{cases} \\ Q_{32}^{i,j} &= \Delta s \begin{cases} -\sin \theta_j, & j < i, \\ 0, & j \geq i, \end{cases} \\ Q_{33}^{i,j} &= 0. \end{aligned}$$

Further, in this parameterisation we may relate the local rate of rotation ω_i about \mathbf{d}_3^i to θ, ϕ, ψ and their time derivatives. Explicitly, this relationship is $\omega = \cos(\theta)\dot{\phi} + \dot{\psi}$, and is notably linear in the derivatives of the Euler angles. Thus, forming the composite matrix

$$\mathcal{Q} = \left[\begin{array}{c|c} \mathcal{Q} & 0 \\ \hline 0 & C \\ \hline 0 & I_N \end{array} \right], \quad (31)$$

where I_N is the $N \times N$ identity matrix and the $N \times N$ matrix C has diagonal elements $C_i = \cos(\theta_i)$ for $i = 1, \dots, N$, with all other elements zero. The $(4N+3) \times (3N+3)$ matrix \mathcal{Q} now encodes the expressions of velocities and rotation rates in terms of the parameterisation, via

$$\mathcal{Q} \dot{\Theta} = \begin{bmatrix} \dot{\mathbf{X}} \\ \boldsymbol{\omega} \end{bmatrix}. \quad (32)$$

Having constructed \mathcal{Q} , we now combine Eqs. (18) and (32) to give

$$-\mathcal{B} \mathcal{A} \mathcal{Q} \dot{\Theta} = \mathbf{R}, \quad (33)$$

noting in particular that the matrix $\mathcal{B} \mathcal{A} \mathcal{Q}$ is square and of dimension $(3N+3) \times (3N+3)$. Naively, this system of ordinary differential equations can be readily solved numerically to give the evolution of the filament in the surrounding fluid. However, the use of a single parameterisation to describe the filament will in general lead to degeneracy of the linear system and ill-defined derivatives in both space and time, issues which we explore and resolve numerically in the next section.

Coordinate singularities

Consider a straight filament aligned with the \mathbf{e}_z axis, with each of the $\mathbf{d}_3^i = [0, 0, 1]^\top$ written in the

laboratory frame. For this filament $\theta_i = 0$ for all i , whilst the ϕ_i are undetermined, arbitrary and notably need not be the same on each segment. Were we to attempt to formulate and solve the linear system of Eq. (33), both ϕ and its derivatives would be ill-defined, and correspondingly we would be unable to solve the system for the filament dynamics, which are otherwise trivial in this particular setup. In more generality, if a filament were to have any segment pass through one of the poles $\theta = \{0, \pi\}$ of this coordinate system, ϕ would be undetermined on the segment and arbitrary, with attempts to solve our parameterised system of ordinary differential equations failing. Further, were a segment to pass close to but not through a pole, time derivatives of ϕ would necessarily become large, with ϕ well-defined but varying rapidly as the segment moves close to the pole of the coordinate system. These large derivatives would artificially introduce additional stiffness to the elastohydrodynamical problem, inherent only to the parameterisation and not the underlying physics. Analogous issues with arclength derivatives occur when considering neighbouring segments, with the value of ϕ varying rapidly and artificially between segments that reside near the pole of the coordinate system. In this latter case however, our formulation of the elastohydrodynamical problem circumvents the need for evaluation of ϕ_s , instead considering only derivatives of the smooth quantities \mathbf{d}_α , though we are not able to resolve issues with temporal derivatives in the same way.

In order to avoid the numerical and theoretical problems associated with singular points in the filament parameterisation, we exploit the finiteness of the set of angles θ_i , along with the independence of the underlying elastohydrodynamical problem from the parameterisation. Throughout this work we have assumed a fixed laboratory frame with basis $\{\mathbf{e}_x, \mathbf{e}_y, \mathbf{e}_z\}$, present only so that vector quantities may be written componentwise for convenience. Our choice of such a basis is arbitrary, with the physical problem of filament motion being independent of our selection of particular basis vectors. It is with respect to this basis that we have defined the Euler angles θ and ϕ , from which the aforementioned coordinate singularities appear if any of the θ_i approach zero or π . Thus, if one makes a choice of basis $\{\mathbf{e}_x^*, \mathbf{e}_y^*, \mathbf{e}_z^*\}$ such that the corresponding Euler angles θ_i^* are some δ -neighbourhood away from the poles of the new parameterisation, the system of ordinary differential equations given in Eq. (33) may be readily solved, at least initially. Should the solution in the new coordinate system approach one of the new poles $\theta^* = 0, \pi$, a new basis can again be chosen, and this process iterated until the filament motion has been captured over a desired interval.

We note that for sufficiently small $\delta > 0$ such a choice of basis $\{\mathbf{e}_x^*, \mathbf{e}_y^*, \mathbf{e}_z^*\}$ necessarily exists due to the finiteness of the set of θ_i , with δ in practice able to be

sufficiently large so as to limit the effects of coordinate singularities. Thus, subject to reasonable assumptions of smoothness of the filament position \mathbf{x} , such a process of repeatedly changing basis when necessary will prevent issues associated with the parameterisation described above, and will in practice enable the efficient simulation of filament motion without introducing artificial stiffness or singularities.

IMPLEMENTATION AND VERIFICATION

Initially choosing a random basis $\{\mathbf{e}_x, \mathbf{e}_y, \mathbf{e}_z\}$, the above formulation is implemented in MATLAB[®], with the system of ordinary differential equations of Eq. (33) being solved using the inbuilt stiff ODE solver `ode15s` [23], making use of variable step sizes in order to satisfy configurable error tolerances that are typically set here at 10^{-7} . Initially and at each timestep, the values of θ_i are checked to determine if they are within δ of a coordinate singularity, typically with $\delta = \pi/30$. Should the parameterisation be approaching a singularity, a new basis is chosen and the problem recast in this basis.

A natural method of selecting a new basis is to choose one uniformly at random. Indeed, by considering the worst-case scenario of the N tuples (θ_i, ϕ_i) uniformly and disjointly covering the surface of the unit sphere, which together θ and ϕ parameterise, the probability that any random basis results in $\min_i \{\theta_i, \pi - \theta_i\} < \delta$ is given by $2N \sin^2(\delta/2)$, a consequence of elementary geometry. With this quantity being significantly less than unity for a wide range of N with δ large enough to avoid severe artificial numerical stiffness, as discussed above, a practical implementation for the simulation of filament elastohydrodynamics as formulated above may simply select a new basis randomly, repeating until a suitable basis is found. With $\delta = \pi/50$ and $N = 50$, the probability of needing to select another basis is bounded above by 10%, thus in practice one should expect to find an appropriate basis within few iterations of the proposed procedure.

However, we may proceed in a deterministic manner, selecting an appropriate basis from knowledge of the existing parameterisation. Given the set of parameters θ_i and ϕ_i , we may choose a $\hat{\theta} \in [0, \pi]$ so as to maximise the distance of $\hat{\theta}$ from the poles $\theta = 0, \pi$ of the existing system, as well as from each of the θ_i and their antipodes, $\pi - \theta_i$. Similarly, we may choose $\hat{\phi} \in (-\pi, \pi]$ so as to maximise the distance from each of the ϕ_i and their antipodes, where distance is measured modulo 2π . With these choices of $\hat{\theta}$ and $\hat{\phi}$, we form a new basis by mapping the original basis vector \mathbf{e}_x to the vector \mathbf{e}_z^* , given explicitly by

$$\mathbf{e}_z^* = [\sin \hat{\theta} \cos \hat{\phi}, \sin \hat{\theta} \sin \hat{\phi}, \cos \hat{\theta}]^\top. \quad (34)$$

Choosing the other orthonormal basis vectors $\mathbf{e}_x^*, \mathbf{e}_y^*$

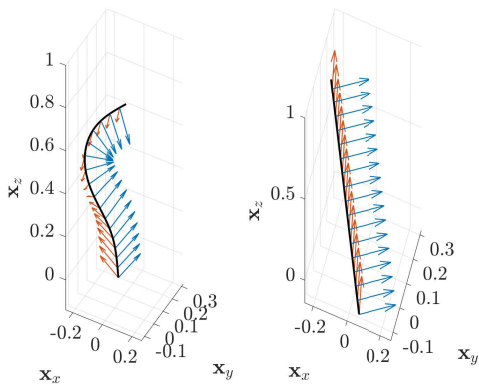


FIG. 1. The relaxation of a filament in three dimensions. Shown are the initial (left) and relaxed (right) configurations of the filament (black, heavy). The vectors \mathbf{d}_α^i are shown as coloured arrows for particular values of i and $\alpha = 1, 2$. We see relaxation from a non-planar, helical-like configuration to a straight filament, with intermediate transients during which the filament untwists and unbends not shown. Here we have simulated with $N = 50$ segments and $\sigma = 1$.

arbitrarily, expressed in this new basis the accompanying filament parameterisation we will be removed from any coordinate singularities, by construction. By considering the ϕ_i and not simply the θ_i alone, we have further increased the separation between the filament parameterisation and coordinate singularities.

Utilising the above deterministic scheme for basis selection, simulations of filament relaxation in three dimensions utilising $N = 50$ segments have an average runtime of approximately 15s on modest hardware (Intel® Core™ i7-6920HQ CPU), typically requiring at most one random choice of basis to avoid singularities in the parameterisation. We see retained in this methodology the low computational cost of the formulation of Moreau *et al.* [16], here extended to filaments in three dimensions and representing significant improvements in computational efficiency over recent studies in three dimensions [14, 15].

Initial verification was performed by comparison to filament relaxation in two dimensions [16–18], along with repeated observation of the relaxation of a variety of initially-curved filaments relaxing in three dimensions to a straight configuration. An example of such a filament and its relaxation to a straight configuration is given in Fig. 1, notably beginning from a helical configuration passing close to the poles of the laboratory-based Euler angle parameterisation of the filament as shown in the figure.

DISCUSSION

We have seen that the motion of inextensible unshearable filaments in three dimensions can be concisely described by an Euler angle parameterisation suitable for efficient numerical solution. Further, we have found that singularities introduced by a choice of coordinate system may be readily circumvented by a change of basis, avoiding artificial numerical stiffness and potential degeneracies in any single parameterisation of the filament. We have extended the two-dimensional methodologies of Moreau *et al.* [16], Walker *et al.* [17], Hall-McNair *et al.* [18] to consider non-planar filaments, and have retained the computational efficiency associated with these previous studies, potentially enabling large-scale exploratory studies of filament dynamics that were previously plagued by severe numerical stiffness.

Though not detailed in this manuscript, the presented framework may readily accommodate hydrodynamics in confined geometries, for example with the inclusion of a planar boundary as in Walker *et al.* [17], in addition to non-trivial background flows, active moments, and complex boundary conditions. Such a framework will enable the study of filament dynamics relevant to biology applications as well as active matter, for example the flagellum of the mammalian spermatozoon.

ACKNOWLEDGEMENTS

We are grateful to Prof. Derek Moulton for discussions on elastic filaments. B.J.W. is supported by the UK Engineering and Physical Sciences Research Council (EPSRC), grant EP/N509711/1. K.I. is supported by JSPS Overseas Research Fellowship (29-0146), MEXT Leading Initiative for Excellent Young Researchers (LEADER), and JSPS KAKENHI Grant Number JP18K13456.

* Corresponding author: benjamin.walker@maths.ox.ac.uk

† ishimoto@ms.u-tokyo.ac.jp

‡ gaffney@maths.ox.ac.uk

- [1] H. C. Berg and R. A. Anderson, Bacteria Swim by Rotating their Flagellar Filaments, *Nature* **245**, 380 (1973).
- [2] J. Gray, *Ciliary movement* (Cambridge University Press, Cambridge [England, 1928]).
- [3] D. J. Smith, T. D. Montenegro-Johnson, and S. S. Lopes, Symmetry-Breaking Cilia-Driven Flow in Embryogenesis, *Annual Review of Fluid Mechanics* **51**, 105 (2019).
- [4] L. Guglielmini, A. Kushwaha, E. S. G. Shaqfeh, and H. A. Stone, Buckling transitions of an elastic filament in a viscous stagnation point flow, *Physics of Fluids* **24**, 123601 (2012).

- [5] M. Roper, R. Dreyfus, J. Baudry, M. Fermigier, J. Bibette, and H. A. Stone, On the dynamics of magnetically driven elastic filaments, *Journal of Fluid Mechanics* **554**, 167 (2006).
- [6] A. K. Tornberg and M. J. Shelley, Simulating the dynamics and interactions of flexible fibers in Stokes flows, *Journal of Computational Physics* **196**, 8 (2004).
- [7] Y. Liu, B. Chakrabarti, D. Saintillan, A. Lindner, and O. du Roure, Morphological transitions of elastic filaments in shear flow, *Proceedings of the National Academy of Sciences* **115**, 9438 (2018).
- [8] C. Pozrikidis, Shear flow over cylindrical rods attached to a substrate, *Journal of Fluids and Structures* **26**, 393 (2010).
- [9] O. du Roure, A. Lindner, E. N. Nazockdast, and M. J. Shelley, Dynamics of Flexible Fibers in Viscous Flows and Fluids, *Annual Review of Fluid Mechanics* **51**, 539 (2019).
- [10] S. F. Schoeller, A. K. Townsend, T. A. Westwood, and E. E. Keaveny, Methods for suspensions of passive and active filaments, , 1 (2019), arXiv:1903.12609.
- [11] M. Maxey and B. Patel, Localized force representations for particles sedimenting in Stokes flow, *International Journal of Multiphase Flow* **27**, 1603 (2001).
- [12] C.-H. Yeung and D. M. Woolley, Three-dimensional bend propagation in hamster sperm models and the direction of roll in free-swimming cells, *Cell Motility* **4**, 215 (1984).
- [13] C. Shingyoji, J. Katada, K. Takahashi, and I. R. Gibbons, Rotating the plane of imposed vibration can rotate the plane of flagellar beating in sea-urchin sperm without twisting the axoneme., *Journal of cell science* **98** (Pt 2), 175 (1991).
- [14] S. D. Olson, S. Lim, and R. Cortez, Modeling the dynamics of an elastic rod with intrinsic curvature and twist using a regularized Stokes formulation, *Journal of Computational Physics* **238**, 169 (2013).
- [15] K. Ishimoto and E. A. Gaffney, An elastohydrodynamical simulation study of filament and spermatozoan swimming driven by internal couples, *IMA Journal of Applied Mathematics* **83**, 655 (2018).
- [16] C. Moreau, L. Giraldi, and H. Gad  lha, The asymptotic coarse-graining formulation of slender-rods, bio-filaments and flagella, *Journal of The Royal Society Interface* **15**, 20180235 (2018).
- [17] B. J. Walker, K. Ishimoto, H. Gad  lha, and E. A. Gaffney, Filament mechanics in a half-space via regularised Stokeslet segments, (2019), arXiv:1904.02543.
- [18] A. L. Hall-McNair, M. T. Gallagher, T. D. Montenegro-Johnson, H. Gad  lha, and D. J. Smith, Efficient Implementation of Elastohydrodynamics via Integral Operators, , 1 (2019), arXiv:1903.03427.
- [19] R. Cortez, Regularized Stokeslet segments, *Journal of Computational Physics* **375**, 783 (2018).
- [20] M. Nizette and A. Goriely, Towards a classification of Euler-Kirchhoff filaments, *Journal of Mathematical Physics* **40**, 2830 (1999).
- [21] A. Chwang and T. Y.-T. Wu, Hydromechanics of low-Reynolds-number flow. Part 1. Rotation of axisymmetric prolate bodies, *Journal of Fluid Mechanics* **63**, 607 (1974).
- [22] S. S. Antman, *Nonlinear Problems of Elasticity*, Applied Mathematical Sciences, Vol. 107 (Springer-Verlag, New York, 2005).
- [23] L. F. Shampine and M. W. Reichelt, The MATLAB ODE Suite, *SIAM Journal on Scientific Computing* **18**, 1 (1997).